Supporting Information

Harnessing Weak Monomer Miscibility to Create Porous Microdomains in Polymer Electrolytes for Zinc-Ion Batteries

Lei Zhang[a,b], Shijun Xiao[b], Xurui Rong[a], Zhiheng Shao[a], Yong Jiang[a], Jiajun Hu[a], Wenyu Wang[a], Gangling Chen[a], Jitao Huang[c,], Qian Wang[d,*], Zhong Jin[c,*], Shi Wang[a,b,c*]*

[a]School of Materials and Chemical Engineering, Chuzhou University, Chuzhou 239099, China.

[b]State Key Laboratory of Flexible Electronics (LoFE) & Institute of Advanced Materials (IAM), Nanjing University of Posts & Telecommunications, 9 Wenyuan Road, Nanjing 210023, China.

[c]State Key Laboratory of Coordination Chemistry, MOE Key Laboratory of Mesoscopic Chemistry, MOE Key Laboratory of High Performance Polymer Materials and Technology, Jiangsu Key Laboratory of Green Energy Catalysis and Intelligent Chemical Engineering, Suzhou Key Laboratory of Green Intelligent Manufacturing of New Energy Materials and Devices, Tianchang New Materials and Energy Technologies Research Center, Institute of Green Chemistry and Engineering, School of Chemistry and Chemical Engineering, Nanjing University, Nanjing, Jiangsu 210023, China.

[d]*College of Materials Science and Engineering, Taiyuan University of Technology, Taiyuan 030024, China.*

E-mail: qianwang0825@pku.edu.cn; zhongjin@nju.edu.cn; iamshiwang@njupt.edu.cn

1. Experimental Section

1.1 Materials

The following reagents were used as received: 2,2,3,4,4,4-hexafluorobutyl acrylate (HFBA, >95.0% GC, Aladdin), acrylamide (AAm, 99.0%, Aladdin), zinc trifluoromethanesulfonate ($Zn(OTf)_2$, 98%, Aladdin), N,N′-methylenebisacrylamide (MBAA, 99%, Aladdin), and 1-hydroxycyclohexyl phenyl ketone (HCPK, 98%, Aladdin). The ionic liquid 1-ethyl-3-methylimidazolium bis(trifluoromethylsulfonyl)imide ([EMIm]TFSI) was used as the primary solvent. All aqueous solutions were prepared using deionized water (18.2 MΩ·cm).

1.2 Materials Characterizations

The chemical composition, functional groups and interaction mechanism of different groups were characterized by Fourier-transform infrared (FTIR) spectroscopy on a Thermo Fisher Nicolet iS50 spectrometer. Surface elemental states were analyzed by X-ray photoelectron spectroscopy (XPS) using a Thermo Scientific K-Alpha instrument, with all binding energies calibrated against the adventitious carbon C 1s peak at 284.80 eV. Crystalline phases were identified via X-ray diffraction (XRD) on a Shimadzu XRD-6100 diffractometer. Morphological analysis was conducted using a Hitachi S4800 field-emission scanning electron microscope (SEM) operated at an accelerating voltage of 5 kV.

1.3 Experimental Procedure

Synthesis of polyacrylamide (PAM) Ionogel Electrolyte

The PAM ionogel was synthesized via UV-initiated polymerization. First, 0.0694 g of AAm was dissolved in 700 μL of [EMIm]TFSI with stirring at 30 °C for 30 minutes. Subsequently, 0.75 g of $Zn(OTf)_2$, a suitable amount of MBAA (crosslinker), and HCPK (photoinitiator) were added to form a homogeneous precursor solution. This solution was then cast into a polytetrafluoroethylene mold or directly onto a zinc foil and irradiated under a 30 W UV lamp for 6 hours, 20 wt% water was further added to yield the PAM ionogel electrolyte, denoted as PAM-IL-Zn.

Synthesis of Amphiphilic (PBAM) Ionogel Electrolyte

The amphiphilic ionogel was prepared following a similar procedure with the addition of the fluorinated monomer. Briefly, 0.0694 g of AAm was dissolved in 700 μL of [EMIm]TFSI at 30 °C for 30 minutes. Then, 166 μL of HFBA was added, and the mixture was stirred for an additional 5 minutes. Following this, varying masses of $Zn(OTf)_2$ (0.5 g, 0.75 g, or 1.0 g), along with the crosslinker and photoinitiator, were introduced to form a clear solution. After UV curing for 6 hours, 20 wt% of water was added to obtain the Poly(AAm-HFBA) ionic gel electrolyte. Samples with different salt contents were designated as PBAM-0.5, PBAM-IL-Zn (with 0.75 g $Zn(OTf)_2$), and PBAM-1.0.

Preparation of $Na_2V_6O_{16}\cdot 3H_2O$ (NVO) Cathode

The NVO cathode material was synthesized hydrothermally. 2.0 g of commercial V_2O_5 powder was added to 30 mL of a 2.0 M NaCl solution and vigorously stirred at room temperature for 96 hours, during which the solution color changed from yellow to brown. The resulting precipitate was collected, thoroughly washed with deionized water and ethanol, and dried at 80 °C for 12 hours. Single-walled carbon nanotubes (SWCNTs) were dispersed in a 0.5 mg mL^{-1} sodium dodecyl sulfate (SDS) aqueous solution via ultrasonication for 30 minutes. The as-synthesized NVO powder was then added to the SWCNT dispersion with a mass ratio of V_2O_5 precursor to SWCNTs of 7:2. After vigorous stirring for 1 hour, the homogeneous slurry was vacuum-filtered to form a freestanding, flexible cathode film. The active material mass loading was approximately 2.0 mg cm^{-2}.

Electrochemical Cell Assembly

All batteries were assembled in CR2032 coin cell configurations using the prepared ionogels as the electrolyte.

Zn||Zn Symmetric Cells: Commercial zinc foil (thickness: 0.1 mm, diameter: 12 mm) was used as both the working and counter electrode. A disc of the PAM-IL-Zn or PBAM-IL-Zn ionogel was sandwiched between two zinc electrodes, and 10 μL of the

water was added to the cell.

Zn||Cu Asymmetric Cells: These cells were assembled using a zinc foil anode, a copper foil cathode (thickness: 0.025 mm, diameter: 12 mm), the ionogel electrolyte, and 10 μL of water.

Zn||NVO Full Cells: Full cells were constructed with a zinc foil anode, the freestanding NVO/SWCNT cathode, the ionogel electrolyte, and 10 μL of water.

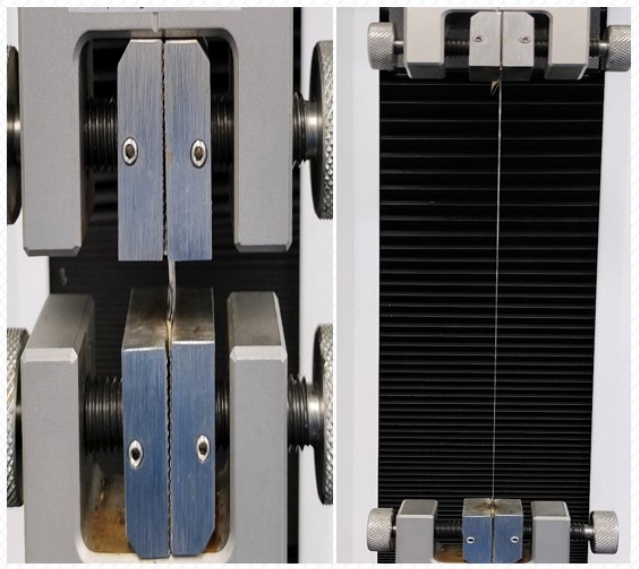

Figure S1. photographs initial and stretched PBAM-IL-Zn.

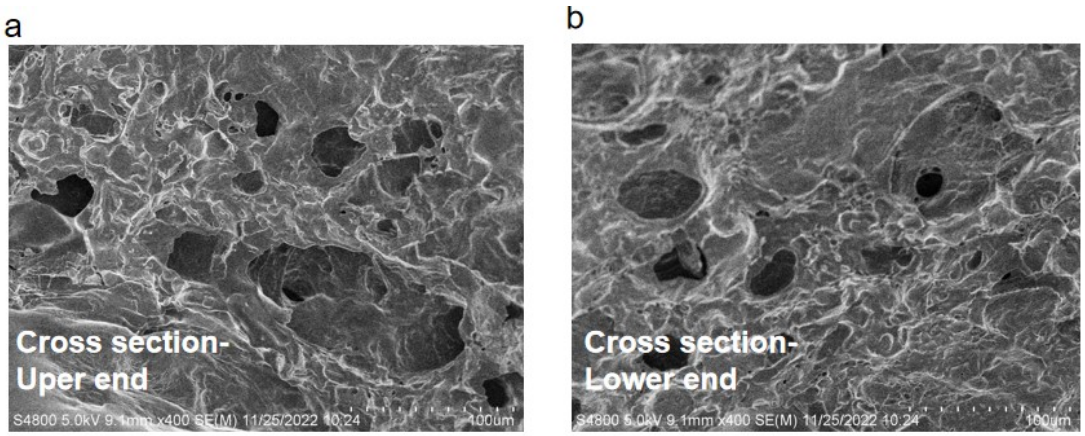

Figure S2. Cross-sectional SEM image of PAM-IL-Zn.

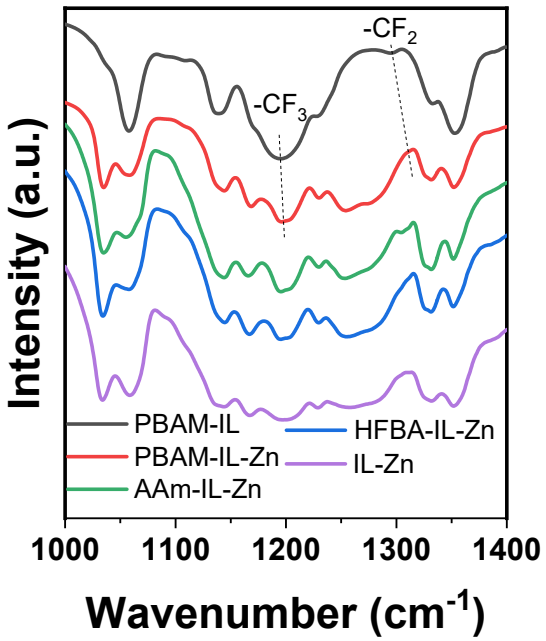

Figure S3. . FTIR characterization of the series of samples.

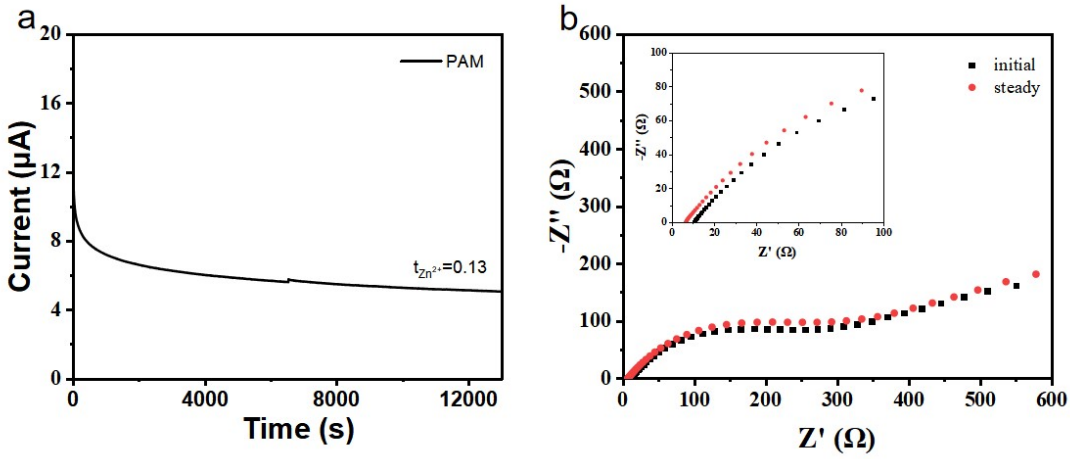

Figure S4. a) Polarization curve and b) EIS profiles before and after polarization for the Zn|PBAM-IL-Zn|Zn symmetric cell.

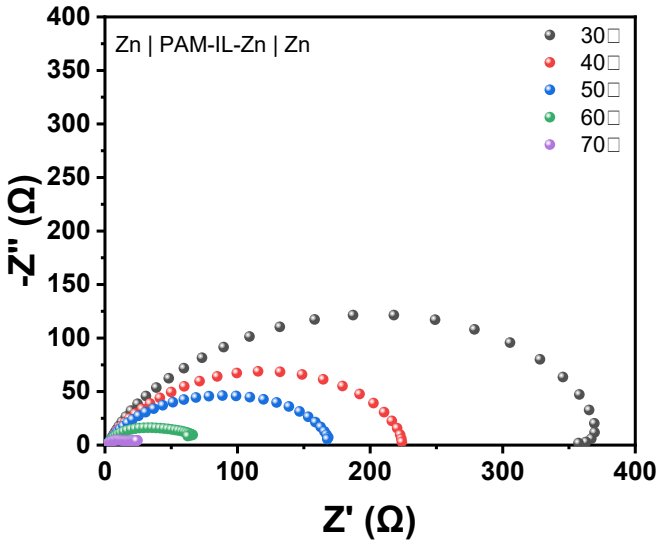

Figure S5. EIS of the Zn|PBAM-IL-Zn|Zn symmetric cell at various temperatures.

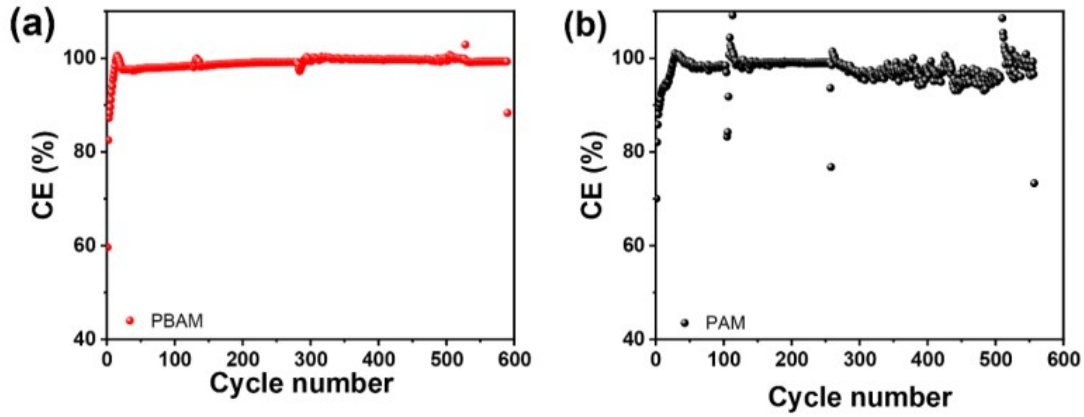

Figure S6. Coulombic Effiiciency of a) PBAM-IL-Zn and b) PAM-IL-Zn based on Zn||Cu cells.

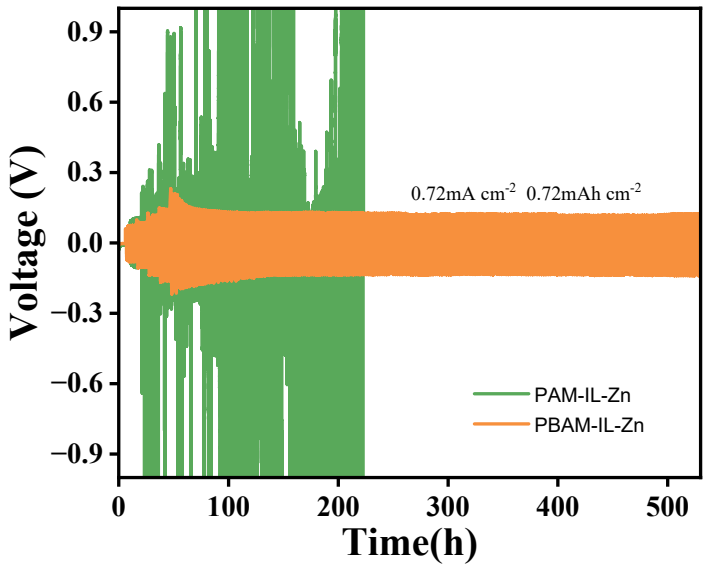

Figure S7. Long-term cycling performance of the Zn||Zn batteries.

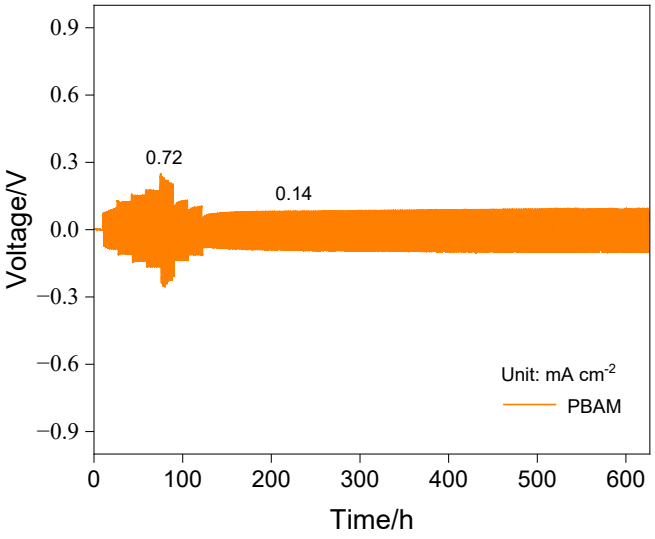

Figure S8. Long-term cycling performance of the Zn||Zn cell using PBAM-IL-Zn

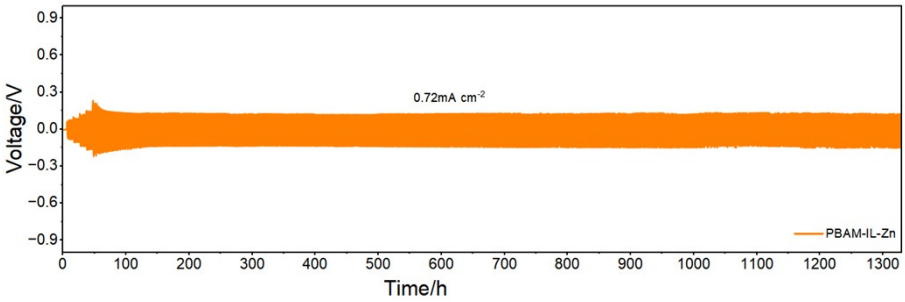

Figure S9. Long-term cycling performance of the Zn||Zn cell using PBAM-IL-Zn

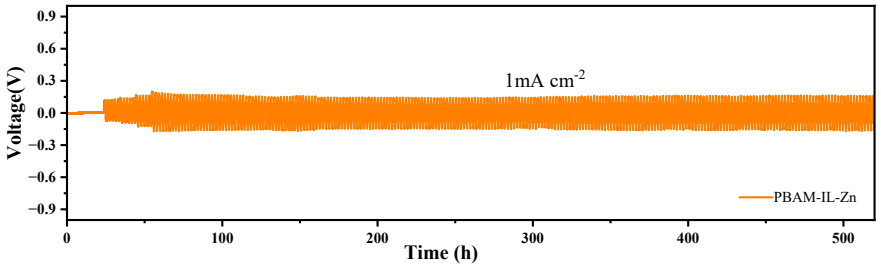

Figure S10. Long-term cycling performance of the Zn||Zn cell using PBAM-IL-Zn

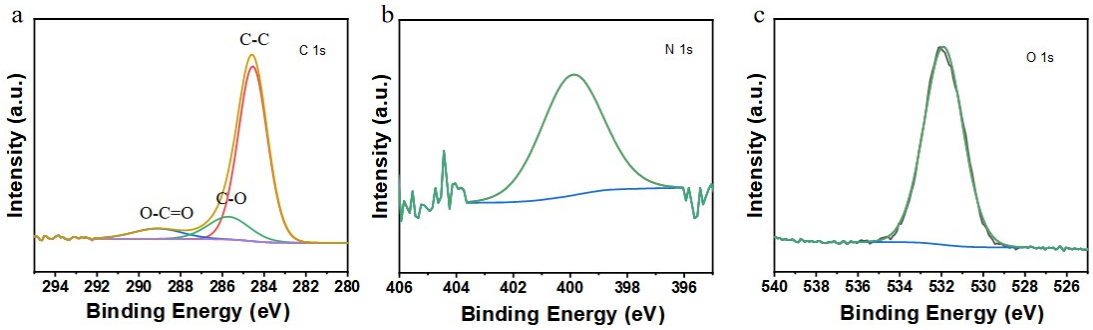

Figure S11. XPS spectra of a) C 1s, b) N 1s and c) N 1s of Zn anode using PAM-IL-Zn